SINGLE-SHOT LONGITUDINAL PHASE SPACE MEASUREMENT DIAGNOSTICS BEAMLINE STATUS AT THE ARGONNE WAKEFIELD ACCELERATOR*

M. Rihaoui[1,2], D. Mihalcea[1], P. Piot[1,3], J. G. Power[2], and W. Gai[2]
[1] Department of Physics, Northern Illinois University DeKalb, IL 60115
[2] High Energy Physics Division, Argonne National Laboratory, Argonne, IL 60439, USA
[3] Accelerator Physics Center, Fermi National Accelerator Laboratory, Batavia, IL 60510, USA

Abstract

A single-shot longitudinal phase space diagnostics experiment is currently being commissioned at the Argonne Wakefield Accelerator (AWA). The diagnostic beamline consists of two magnetic dipoles that bend the beam horizontally followed by an rf deflecting cavity that streaks the beam vertically. Using this configuration, the incoming longitudinal phase space can be mapped to a final (x, y) plane which can be directly measured, e.g., using a YAG screen. In this paper we discuss the performances of such longitudinal phase space diagnostics and present its experimental status.

INTRODUCTION

Many advanced-acceleration and light-source concepts rely on the production of bright electron beams. Diagnosing these beams with unprecedented parameters can be challenging. In this paper we discuss the design and construction of a single-shot longitudinal phase space (LPS) diagnostics about to be commissioned at the Argonne Wakefield Accelerator (AWA) [1]. A transverse-to-longitudinal phase space exchange (PEX) experiment has been proposed as a mean to shape the electron beam's current distribution. In this scheme a horizontally-deflecting cavity is flanked by two dispersive sections arranged as doglegs [2, 3]. As a first step toward building this PEX beamline, we have installed the upstream dogleg and a transverse deflecting cavity (TDC); see Fig. 1. In its present configuration, the TDC deflects the beam vertically thereby providing an opportunity for single-shot LPS measurement while commissioning and characterizing the key components of the PEX beamline. In the constructed "LPS beamline", the initial LPS coordinates (z_0, δ_0) are mapped to the transverse plane (x, y) while minimizing other correlation terms. Therefore the method can image the initial LPS distribution on a transverse screen located downstream of the TDC. Similar experiments have recently been performed at other facilities [4, 5]. In our configuration, the dispersive section is upstream of the TDC; see Fig. 1. The TM_{110}-like TDC operates at 1.3 GHz and consists of 1/2-1-1/2 cells [6]. The TDC is nominally operated at the zero-crossing phase of the field so that the head and tail of the bunch are subject to opposite transverse momentum kicks thereby streaking the beam [7].

*This work is supported by the US DOE under Contract DE-FG02-08ER41532 with Northern Illinois University and under Contract No. DE-AC02-06CH11357 with Argonne National Laboratory.

The LPS beamline is located downstream of the AWA's main beamline, after the beam, produced in an L-band rf-gun, has been accelerated to $\sim$ 15 MeV in a 1.3-GHz booster cavity. The simulations presented below start at $s = 2.79$ m from the photocathode and the transport line to the first dipole magnet (D1 located at $s \simeq 5.4$ m) includes a solenoid (at $z \simeq 3.1$ m) that provide some control over the transverse Courant-Snyder (C-S) parameters upstream of the LPS diagnostics beamline.

BEAMLINE DESIGN

The LPS beamline consists of two magnetic dipoles, an rf transverse deflecting cavity, three quadrupoles and three YAG screens. The dogleg horizontally disperses the beam so that the horizontal position downstream is $x(s) = \eta_x(s)\delta_0 + h_x$ where $\eta_x(s)$ is the horizontal dispersion function at the axial location s, δ_0 is the initial fractional energy spread, and h_x is a quantity that includes

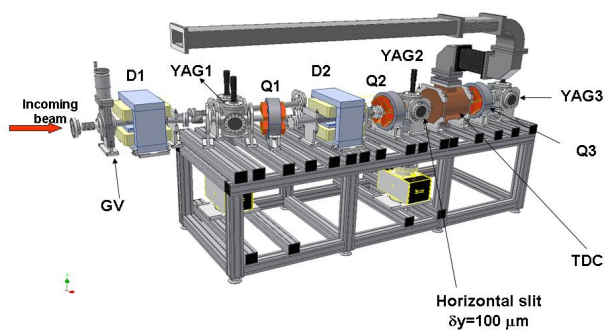

Figure 1: 3D rendition of the single-shot LPS diagnostics. GV is the gate valve, Q1, Q2, Q3 represent the quadrupoles, YAG1,YAG2, and YAG3 are the YAG screens, D1, D2 are dipoles, and TDC is the transverse deflecting cavity. [Courtesy of S. Doran (AWA)]

other contributions (such as initial emittance). The TDC deflects the electron beam vertically and the beam position downstream of the TDC is related to the longitudinal coordinate upstream of the TDC, z_c, via $y = \kappa z_c + h_y$ where $\kappa \equiv (2\pi/\lambda)|e|V_y/\mathcal{E}$ is the TDC's normalized deflecting strength (here e is the electronic charge, $\lambda \simeq 0.23$ m is the free-space rf wavelength, V_y the deflecting voltage, and $\mathcal{E}$ the beam's energy [8, 9]. In the latter equation, h_y describes the contribution from other initial coordinates. If the dogleg is made achromatic then $z_c = z_0$ (where z_0 is the longitudinal position upstream of the LP beamline) and under linear and single-particle-dynamics approximations, the longitudinal emittance upstream of the LPS can be inferred from

$$\epsilon_{z_0}^2 = \left(\frac{\beta\gamma}{\eta\kappa}\right)^2 [\langle x^2\rangle\langle y^2\rangle - \langle xy\rangle^2 + H_{x_0,y_0}],$$

where γ is the Lorentz factor and $\beta \equiv (1 - 1/\gamma^2)^{1/2}$ and $H_{x_0y_0}$ is a resolution-limiting term depending on the initial transverse emittances.

The quadrupole magnet Q1 controls the longitudinal dispersion R_{56} of the dogleg and can especially be use to set the dogleg achromatic ($R_{56} = 0$), doing so also sets the downstream dispersion. The quadrupoles Q2 and Q3 are tuned to insure the beam spot on YAG3 is dominated horizontally by the dispersion term ($\eta_x\delta_0$) and vertically by the streaking term (κz_0). Finally, two horizontal slits are used in the setup. A first slit, with variable vertical gap, located upstream of the LPS diagnostics beamline, samples the beam thereby mitigating space charge effects in the LPS beamline. A second slit with 100-μm vertical gap, located upstream of the TDC, limits the vertical beam size throughout the TDC and minimize possible energy spread dilution due to the dependency of the axial electric field on the vertical coordinate (in the paraxial approximation $E_z \propto y$ for the TM_{110} mode).

SINGLE-PARTICLE DYNAMICS

Single-particle-dynamics simulations of the LPS beamline were performed with the tracking program ELEGANT [10]. The simulations start downstream of the booster cavity and include a solenoid location ~ 1.4 m upstream of the LPS beamline. We consider the case of a 100-pC bunch with initial C-S parameters $(\alpha_{x,y}, \beta_{x,y})$=(-10.5, 10.7 m) and transverse normalized emittances $\varepsilon_{n,x,y} = 0.87$ μm. The dogleg is set so that its R_{56} vanishes, resulting at D2 exit, in a dispersion vector (η_x, η_x')=(0.13 m, 1.11) where $\eta_x' \equiv d\eta_x/ds$ is the dispersion slope.

We employ an iterative procedure to devise the settings of the quadrupoles Q2 and Q3 (which control the betatron functions and horizontal dispersion at YAG3) and of the upstream solenoid. We first turn off the TDC and vary the magnetic field $\hat{B}_z$ of the upstream solenoid. For each setting, the strength of Q2 and Q3 are varied within the permissible ranges. An example of such a scan (for $\hat{B}_z = 0.175$ T) is depicted in Fig. 2. The locus of optimum setting corresponds to values where the transverse rms beam size is dominated by dispersion while maintaining a small vertical beam size.

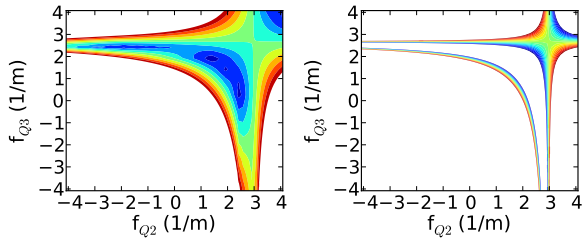

Figure 2: Horizontal rms beam size σ_x (left) and dispersion η_x (right) as function of quadrupoles Q2 and Q3 focal length. Only values of $0 < \sigma_x < 10$ mm and $030 < |\eta_x| < 50$ m are shown [with lower (resp. upper) values corresponding to blue (resp. red)]

To assess detrimental effects limiting the imaging of the LPS onto the transverse plane at YAG3, we take an initial transversely-Gaussian macroparticle distribution with the same C-S parameters as above. The initial LPS is populated so that macroparticles are located on the lines of a two-dimensional grid of the form

$$\Phi(z_0, \delta_0) = \sum_i \delta(\delta_0 - i\Delta\delta_0) \sum_j \delta(z_0 - j\Delta z_0),$$

where $\delta()$ is the Dirac function, i and j are indices than span negative and positive values and $\Delta\delta_0$ and Δz_0 are the grid line separation along the two LPW axis; see top plot in Fig. 3. The distribution is then tracked in the LPS beamline using the settings devised previously [here we take (f_{Q2}, f_{Q3})=(1 m^{-1}, 1 m^{-1})].

The final transverse distribution at YAG3 location appears on the bottom plots shown in Fig. 3 for the two zero-crossing phases of the TDC. The local blurring of the grid lines observed at YAG3 comes from the finite (non-vanishing) values of the horizontal and vertical betatron functions while the curvature of the overall distortion is a consequence of second order effects (chromatic aberrations). Therefore, measurements of the transverse distribution for the two zero crossing of the TDS are required for an accurate reconstruction of the initial LPS.

MULTI-PARTICLE SIMULATIONS

Cathode-to-YAG3 multi-particle simulations using 100k macroparticles were performed with the particle-in-cell tracking code IMPACT-T [11].

When the normalized deflection strength of the TDC is set at $\kappa = 3.7$ m^{-1}, the simulations indicate that the longitudinal-to-vertical calibration factor at YAG3 is $C_{yz} = 3.31$ mm/mm (or 0.96 mm/ps) while calibration of

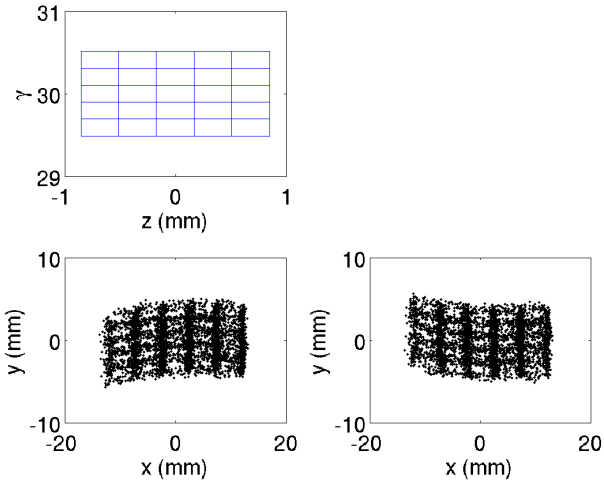

Figure 3: Initial LPS (top plot) and transverse distribution for the two zero-crossing phases of the TDC (bottom plots).

the horizontal axis as a function of fractional energy spread is $C_{x\delta} = 17.40$ mm/%. These values agree well with the ones obtained by another method [12]. Taking the optical resolution of the YAG3 imaging system to be 40 μm in both direction, the above calibration factors would translate in an instrumental resolution of 12 μm (or 40 fs) and 2×10^{-3} for respectively the longitudinal (or time) and fractional energy spread measurements.

Figure 4 shows the initial LPS distribution (z_0, δ_0) before the first dipole and the final distribution transverse (x, y) at YAG3. One of the complications we observe is the presence of correlation between δ_0 and the transverse initial coordinates (x_0, y_0). Therefore the slit upstream D1 also acts as an energy filter (particle with large y_0 tend to be at larger value of δ_0).

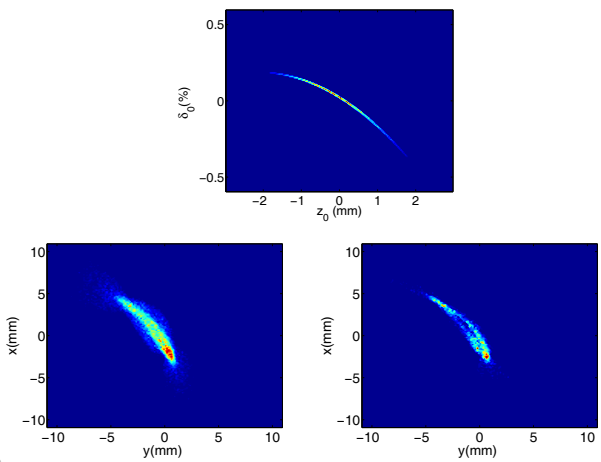

Figure 4: LPS upstream of the diagnostics beamline (top left) and beam's transverse density distributions on YAG3 without (bottom left) and with (bottom right) the two horizontal slits inserted in the beamline.

STATUS & FUTURE WORK

The LPS diagnostics described in this paper has been installed at AWA and will be commissioned within the next few week. Figure 5 shows the current beamline at the end of the existing AWA beamline. We plan on using this diagnostics to explore velocity bunching and investigate the evolution of the LPS associated to high-charge electron bunches.

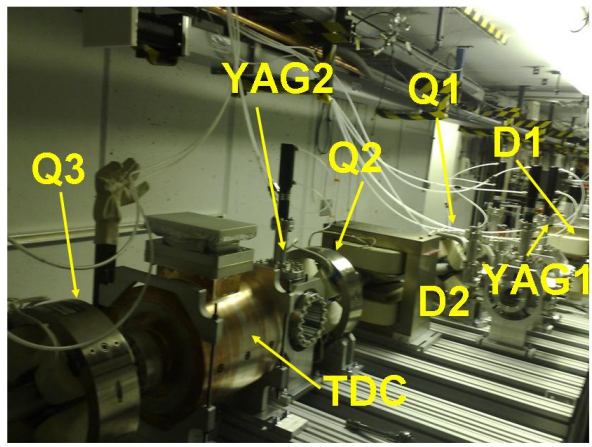

Figure 5: Photograph of the current experimental setup. The YAG3 screen (not shown) is located downstream of the quadrupole Q3 on the lower left of the picture.

REFERENCES

[1] Information on the Argonne Wakefield Facility are available at `http://gate.hep.anl.gov/awa`.

[2] M. Rihaoui, *et al.*, Proceedings of PAC09, 3907 (2009).

[3] P. Piot, *et al.*, Phy. Rev. ST AB **14**, 022801 (2011).

[4] J. T. Moody, *et al.*, Phy. Rev. ST AB **12**, 070704 (2009).

[5] C. Behrens, *et al.*, Proceedings of FEL09, 599 (2009).

[6] J. Shi, *et al.*, Nucl. Instr. Meth. **A598**, 388 (2008).

[7] R.Akre, *et al.*, Proceedings of EPAC 2002, 1882 (2002).

[8] M. Cornacchia and P. Emma, Phy. Rev. ST AB **5**, 084001 (2002).

[9] D. A. Edwards, "Notes on transit in deflection mode pillbox cavity", unpublished (2007).

[10] M. Borland, ANL/APS note LS-287 (2000).

[11] J. Qiang, *et al.*, Phy. Rev. ST AB **9**, 044204 (2006).

[12] M. Rihaoui, *et al.*, in *Advanced Accelerator Concepts*, AIP Proceedings **1299**, 570 (2010).